Diffusive magnonic spin transport in antiferromagnetic insulators

S. M. Rezende,[1,*] R. L. Rodríguez-Suárez,[1,2] and A. Azevedo[1]

[1]*Departamento de Física, Universidade Federal de Pernambuco, 50670-901, Recife, Pernambuco, Brazil*
[2]*Facultad de Física, Pontificia Universidad Católica de Chile, Casilla 306, Santiago, Chile*

It has been shown recently that a layer of the antiferromagnetic insulator (AFI) NiO can be used to transport spin current between a ferromagnet (FM) and a nonmagnetic metal (NM). In the experiments one uses the microwave-driven ferromagnetic resonance in a FM layer to produce a spin pumped spin current that flows through an AFI layer and reaches a NM layer where it is converted into a charge current by means of the inverse spin Hall effect. Here we present a theory for the spin transport in an AFI that relies on the spin current carried by the diffusion of thermal antiferromagnetic magnons. The theory explains quite well the measured dependence of the voltage in the NM layer on the thickness of the NiO layer.

I. INTRODUCTION

The continuing discovery of new processes and materials to generate, transport, and detect spin currents has been driving the field of spintronics to possibilities not imaginable one decade ago [1,2]. Nowadays spin currents are routinely generated by means of the spin Hall effect (SHE) [3–6], ferromagnetic resonance (FMR) driven spin pumping [7–10], and spin Seebeck effect (SSE) [11–16]. Detection of spin currents is usually done through their conversion into charge currents by means of the inverse spin Hall effect (ISHE) [3,5,6,10] or the inverse Rashba-Edelstein effect (IRRE) [17–20], and also by the spin-transfer torque exerted on the magnetization of attached magnetic layers [21,22].

Spin current phenomena were initially studied with non-magnetic metals (NMs), in which a pure spin current consists of electrons with opposite spins moving in opposite directions [1,2,23]. Nonmagnetic metals with large spin-orbit interaction, such as Pt, were then widely used to generate and detect spin currents by the ISHE and SHE, and also to transport spin information [1,2,5,6]. It was early recognized that the transport mechanism is the diffusion of spin accumulation generated by some process, such as spin pumping at the interface with a ferromagnet under FMR [5–8]. Later it was discovered that spin currents could also flow in the insulating ferrimagnet yttrium iron garnet (YIG) with the advantage of not having Joule losses [24]. This gave rise to the areas of magnon spintronics and insulator spintronics, in which the carriers of spin information are magnons, the quanta of spin waves [25,26].

Antiferromagnetic (AF) materials, on the other hand, have had a minor role in spintronics. They are essential in the most important spintronic device, namely spin-valve reading heads employed in all hard-disk drives. But they only have a passive role of pinning the magnetization of the reference magnetic layer by means of the interfacial exchange bias [27–29]. However, it has been predicted that, due to some unique dynamic features, AF materials might have applications in novel devices [30]. In fact, recent discoveries of SHE [31,32], SSE [33,34], and spin transport [35–38] in antiferromagnets have largely increased the possibilities of

using AF materials for signal processing making possible the field of antiferromagnetic spintronics [39–45].

Spin transport in antiferromagnetic insulators (AFIs) has been largely overlooked, probably because these materials have vanishing net magnetization. However, recently three groups independently demonstrated unequivocally [35–38] that a spin current can flow through NiO, a room-temperature AFI widely used for exchange biasing in spin valves. Two experiments were done with similar YIG/NiO/Pt trilayer structures where a spin current was generated by spin pumping through microwave-driven FMR in the YIG layer. The pumped spin current flows through the NiO layer and reaches the Pt layer where it is converted into a charge current by the ISHE. Recently two theoretical models have been proposed for the spin transport in FM/AFI/NM trilayers [46,47]. Both are based on the coherent magnetization dynamics in antiferromagnets but none of them explain quantitatively the experimental results in YIG/NiO/Pt trilayers [35–37]. In this paper we present a theory for the spin transport in AFI based on the diffusion of thermal antiferromagnetic magnons. The theory explains the distinctive initial increase and the peak in the voltage with increasing AFI thickness followed by an exponential decay. The model is applied to YIG/NiO/Pt structures and is shown to be in good quantitative agreement with the experimental data of Refs. [35–37].

II. DIFFUSIVE MAGNONIC SPIN TRANSPORT

We consider the FM/AFI/NM trilayer structure illustrated in Fig. 1, which corresponds to the configuration used in the experiments of Refs. [35–37], to demonstrate spin transport through antiferromagnetic insulators. The precessing spins in the FM layer, undergoing microwave-driven FMR, generate a spin current at the FM/AFI interface by the spin pumping process. The spin pumping into the AFI is made possible by the interface exchange interaction between the spins in the FM and in the AFI. The pumped spin current is carried by magnons in the AFI and flows into the NM layer, where it is converted into a charge current by the ISHE making possible the electric detection. In this section we discuss the process by which the spin current is transported in the AFI while the boundary-value problem in the trilayer is presented in Sec. III. As we remarked in the Introduction, it has been proposed that the spin transport in the AFI takes place by means
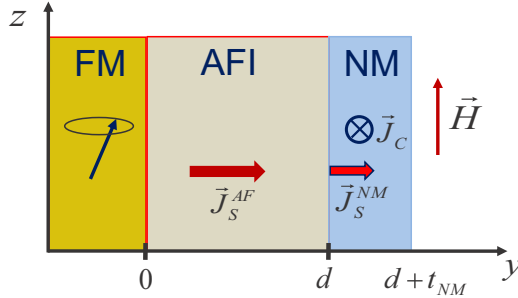
---

*rezende@df.ufpe.br

FIG. 1. Illustration of the ferromagnet (FM)/antiferromagnetic insulator (AFI)/nonmagnetic metal (NM) trilayer structure employed to investigate the spin transport in the AFI, showing the coordinate axes, the AF magnon spin current produced by the spin pumping in the FM/AFI interface, the spin current in the NM layer, and the charge current generated by the ISHE.

of coherent magnetization dynamics [46,47]. Alternatively, we consider here that the mechanism of spin current is the diffusion of incoherent thermal magnons due to the gradient in the concentration of the magnon accumulation produced by the spin pumping in the FM/AFI interface. This mechanism is similar to the diffusion of spin accumulation that occurs in a NM layer under spin pumping in a FM/NM interface [7,8].

We consider a two-sublattice antiferromagnet with quantized spin-wave excitations represented by the Hamiltonian

$$H = \sum_k \hbar(\omega_{\alpha k}\alpha_k^\dagger \alpha_k + \omega_{\beta k}\beta_k^\dagger \beta_k), \quad (1)$$

where $\alpha_k^\dagger$, α_k and $\beta_k^\dagger$, β_k are the creation, annihilation operators of the two normal magnon modes α and β with wave number k and frequencies $\omega_{\alpha k}$ and $\omega_{\beta k}$. In Eq. (1) $\alpha_k^\dagger \alpha_k$ and $\beta_k^\dagger \beta_k$ represent the number operators of magnons of each mode. In easy-axis antiferromagnets, such as MnF_2, FeF_2, and Cr_2O_3, in equilibrium the spins of the two sublattices point in opposite directions along the easy axis. Each magnon mode involves excitations of both sublattice spins and in the absence of an applied magnetic field the two frequencies are the same [48,49]. By applying a field in the easy-axis direction the frequency of one mode increases linearly with the field intensity while the other decreases. If the field exceeds a critical value the frequency of the downgoing mode becomes negative and there is a transition to the spin-flop phase, with the spin vectors pointing nearly in opposite directions and approximately perpendicular to the field. In hard-axis antiferromagnets, such as MnO and NiO, in equilibrium the spins of the two sublattices lie in opposite directions in the plane perpendicular to the axis and point along the in-plane easy-axis anisotropy. In this case also the two magnon modes involve excitations of both spins but even in the absence of an external field the two frequencies are different, as shown in Appendix A. In both cases the frequencies of the two magnon modes are minimum at the center of the Brillouin zone, $k = 0$, and increase as k increases, reaching the maximum values at the Brillouin zone boundary. The calculation of the magnon frequencies for MnF_2 and FeF_2 is in Ref. [49] and for the room-temperature antiferromagnet NiO is presented in Appendix A.

As shown in Appendix B, in both types of antiferromagnets considered here the spin current is carried by the two magnon modes and the z-polarized spin current density operator can be written as

$$\vec{J}_S^z = \frac{\hbar}{V} \sum_k [-\vec{v}_{\alpha k}\alpha_k^\dagger \alpha_k + \vec{v}_{\beta k}\beta_k^\dagger \beta_k], \quad (2)$$

where $\vec{v}_{\mu k} = \hat{k}\partial\omega_{\mu k}/\partial k$ is the group velocity of mode μ and V is the volume of the AFI layer. The spin currents carried by two magnon modes have opposite directions, so that if they have the same group velocity and the same magnon number, the net spin current vanishes in antiferromagnets [49,50]. This is the case of MnF_2, FeF_2, and Cr_2O with no external magnetic field. On the other hand, in NiO the two magnon modes have different frequencies near the Brillouin zone center so that the net spin current can be nonzero in the absence of external field.

Following the work of Zhang and Zhang [51,52] for ferromagnetic insulators, we introduce here the concept of magnon accumulation in an AFI and show that a gradient in its concentration produces magnon diffusion with an associated spin current. Denote by $n_{\mu k}(\vec{r})$ the number of magnons in the $\mu = \alpha, \beta$ mode with wave number k at a position $\vec{r}$ in the AFI layer, $n_{\mu k}^0$ the number in thermal equilibrium, given by the Bose-Einstein distribution,

$$n_{\mu k}^0 = \frac{1}{e^{\hbar\omega_{\mu k}/k_B T} - 1}, \quad (3)$$

and $\delta n_{\mu k}(\vec{r}) = n_{\mu k}(\vec{r}) - n_{\mu k}^0$ the number in excess of equilibrium. Since $\sum_k n_{\mu k}^0 \vec{v}_{\mu k} = 0$, with Eq. (2) we can write the magnon spin current carried by thermal magnons in excess of equilibrium as

$$\vec{J}_S^z = \frac{\hbar}{V} \sum_k \vec{v}_{\alpha k}[-(n_{\alpha k}(\vec{r}) - n_{\alpha k}^0) + \rho_k(n_{\beta k}(\vec{r}) - n_{\beta k}^0)], \quad (4)$$

where $\rho_k = v_{\beta k}/v_{\alpha k}$ is a coefficient expressing the ratio between the group velocities of the two modes. We define the effective magnon accumulation $\delta n_m(\vec{r})$ for the AFI as the density of the effective number of magnons in excess of equilibrium

$$\delta n_m(\vec{r}) = \frac{1}{V} \sum_k \left\{ -[n_{\alpha k}(\vec{r}) - n_{\alpha k}^0] + \rho_k[n_{\beta k}(\vec{r}) - n_{\beta k}^0] \right\}. \quad (5)$$

The distribution of the magnon number under the influence of a thermal gradient can be calculated with the Boltzmann transport equation [51–54]. In the absence of external forces and thermal gradient, in the relaxation approximation and steady state, the Boltzmann equation gives for each magnon mode

$$n_{\mu k}(\vec{r}) - n_{\mu k}^0 = -\tau_{\mu k}\vec{v}_{\mu k} \cdot \nabla[n_{\mu k}(\vec{r}) - n_{\mu k}^0], \quad (6)$$

where $\tau_{\mu k}$ is the μk-magnon relaxation time. Using Eq. (6) in Eq. (4) and approximating the sums by integrals over the Brillouin zone one can show that the spin current density due to gradients in the magnon concentrations in excess of equilibrium is

$$\vec{J}_S^z = -\frac{\hbar}{(2\pi)^3} \int d^3k \left[\tau_{\alpha k}\vec{v}_{\alpha k}\vec{v}_{\alpha k} \cdot \nabla \delta n_{\alpha k} \right.$$
$$\left. - \tau_{\beta k}\vec{v}_{\beta k}\vec{v}_{\beta k} \cdot \nabla \delta n_{\beta k} \right]. \quad (7)$$

In order to calculate the spin current due to the gradient of magnon accumulation, one needs to relate the integral in Eq. (7) with $\delta n_m(\vec{r})$ in Eq. (5). For simplicity we assume variation only in the y direction in the coordinate system in Fig. 1. We consider for the solution of the Boltzmann equation expansions of the nonequilibrium magnon distribution for each mode as [54,55]

$$n_{\mu k}(\vec{r}) = n_{\mu k}^0 + n_{\mu k}^0 \varepsilon_{\mu k} g(y), \tag{8}$$

where $\varepsilon_{\mu k} = \hbar \omega_{\mu k}$ is the magnon energy, T the temperature, and $g(y)$ a spatial distribution to be determined by the solution of the boundary-value problem. With Eq. (8) the magnon accumulation in Eq. (5) becomes

$$\delta n_m(y) = \frac{1}{(2\pi)^3} \int d^3 k \big[-n_{\alpha k}^0 \varepsilon_{\alpha k} + \rho_k n_{\beta k}^0 \varepsilon_{\beta k} \big] g(y), \tag{9}$$

so that one can write $\delta n_m(y) = (-I_{0\alpha} + I_{0\beta}) g(y)$, where

$$I_{0\alpha} = \frac{1}{(2\pi)^3} \int d^3 k n_{\alpha k}^0 \varepsilon_{\alpha k}$$

$$\text{and} \quad I_{0\beta} = \frac{1}{(2\pi)^3} \int d^3 k \rho_k n_{\beta k}^0 \varepsilon_{\beta k}. \tag{10}$$

Using Eqs. (9) and (10) in Eq. (7) we can write the magnonic diffusion spin current as

$$J_S^z(y) = -\hbar D_m \frac{\partial \delta n_m(y)}{\partial y}, \tag{11}$$

where

$$D_m = \frac{1}{(2\pi)^3 (I_{0\beta} - I_{0\alpha})} \int d^3 k \cos^2 \theta$$

$$\times \big[-v_{\alpha k}^2 \tau_{\alpha k} n_{\alpha k}^0 \varepsilon_{\alpha k} + v_{\beta k}^2 \tau_{\beta k} n_{\beta k}^0 \varepsilon_{\beta k} \big] \tag{12}$$

is the diffusion coefficient that can be calculated for a specific AFI by integration over the Brillouin zone. Considering that the magnon accumulation relaxes into the lattice with magnon-phonon relaxation time τ_{mp}, conservation of angular momentum implies that

$$\frac{\partial J_S^z}{\partial y} = -\hbar \frac{\delta n_m}{\tau_{mp}}. \tag{13}$$

Using this relation in Eq. (11) we obtain a diffusion equation for the magnon accumulation that has the same form as in a ferromagnet [51–54],

$$\frac{\partial^2 \delta n_m(y)}{\partial y^2} = \frac{\delta n_m(y)}{l_m^2}, \tag{14}$$

where $l_m = (D_m \tau_m)^{1/2}$ is the magnon diffusion length. Considering that the magnon accumulation is created only by the spin pumping current, the solution of Eq. (14) is

$$\delta n_m(y) = A \sinh(y/l_m) + B \cosh(y/l_m), \tag{15}$$

where A and B are coefficients to be determined by the boundary conditions. The y component of the z-polarized magnon spin current in the AFI, calculated with Eqs. (11) and (15), is

$$J_S^z(y) = -\hbar \frac{D_m}{l_m} A \cosh(y/l_m) - \hbar \frac{D_m}{l_m} B \sinh(y/l_m). \tag{16}$$

Using Eqs. (15) and (16) one can obtain expressions for the magnon accumulation and the spin current density at an arbitrary position y in terms of the spin currents at the two sides of the AFI layer,

$$\delta n_m(y) = \frac{l_m / \hbar D_m}{\sinh(d/l_m)} \big\{ J_S^z(0) \cosh[(y-d)/l_m]$$

$$- J_S^z(d) \cosh(y/l_m) \big\}, \tag{17}$$

$$J_S^z(y) = -\frac{1}{\sinh(d/l_m)} \big\{ J_S^z(0) \sinh[(y-d)/l_m]$$

$$- J_S^z(d) \sinh(y/l_m) \big\}. \tag{18}$$

Equations (17) and (18) will be used in the next section for matching the boundary conditions at the two interfaces.

III. MAGNONIC SPIN CURRENT IN A FM/AFI/NM TRILAYER

In this section we consider the FM/AFI/NM trilayer of Fig. 1 and calculate the spin current density at the AFI/NM interface that flows through the AFI layer, reaches the NM layer, and gives origin to the charge current and the voltage measured in the experiments. For this we use the boundary conditions at $y = 0$ and $y = d$ given by the continuity of the spin current at the interfaces, $J_S^z(0^-) = J_S^z(0^+)$ and $J_S^z(d^-) = J_S^z(d^+)$ [8,56].

At the FM/AFI interface the spin current is produced by spin pumping from the precessing magnetization $\vec{M}$ in the FM layer, driven by the microwave field. The spin current density pumped at the interface is [7,8] $\vec{J}_S^{sp}(0,t) = (\hbar/4\pi M^2) g_{1r}^{\uparrow\downarrow} (\vec{M} \times d\vec{M}/dt)$, where $g_{1r}^{\uparrow\downarrow}$ is the real part of the spin-mixing conductance of the FM/AFI interface, in units of area^{-1}. The z component of the spin current flowing in the y direction has a dc contribution, given by the time average of $\vec{J}_S^{sp}(0,t)$, $J_S^{sp}(0) = (\hbar \omega g_{1r}^{\uparrow\downarrow}/4\pi M^2) \mathrm{Im}(m_x^* m_y)$, where m_x and m_y are the amplitudes of the transverse components of the magnetization. In this equation and hereafter, for simplicity, we omit the superscript z indicating the direction of spin polarization. Using the expressions for the rf susceptibility one can show that the spin current pumped at the FM/AFI interface is [57]

$$J_S^{sp}(0) = \frac{\hbar \omega p g_{1r}^{\uparrow\downarrow}}{4\pi} \left(\frac{h}{\Delta H} \right)^2 L(H - H_R), \tag{19}$$

where h is the amplitude of the driving rf field; ΔH and H_R are, respectively, the linewidth and field for resonance of the FM layer at the frequency ω; $L(H - H_R)$ is the Lorentzian line shape; and p is the precession ellipticity. In order to find the net spin current flowing into the AFI one has to calculate the backflow spin current produced by the spin excitations in the AFI. Since the FMR frequency is typically orders of magnitude smaller than the magnon frequencies in the AFI, the backflow current is not produced by coherent excitations in the AFI. Instead, we consider that it is due to spin pumping by the spin precessions associated with the magnon accumulation at $y = 0^+$ corresponding to the thermal magnons in excess of equilibrium with all frequencies in the Brillouin

zone. The spin pumping from coherent spin precession in antiferromagnets has been calculated in Ref. [58] using a semiclassical approach. In Appendix B we show that the spin current produced by spin pumping from the magnon accumulation is given by

$$J_S^{bf}(0) = b\hbar g_{1r}^{\uparrow\downarrow} \delta n_m(0), \qquad (20)$$

where b is a factor involving integrations over the Brillouin zone given by Eq. (B11).

As we will show later, the backflow spin current in Eq. (20) can be written as $J_S^{bf}(0) = \beta g_{1r}^{\uparrow\downarrow} J_S(0)$, where β is a backflow factor and $J_S(0)$ is the net spin current at the FM/AFI interface flowing into the AFI, given by $J_S(0) = J_S^{sp}(0) - J_S^{bf}(0)$. With these relations and Eq. (19) one can write the net spin current pumped into the AFI as

$$J_S(0) = (g_{1\text{eff}}^{\uparrow\downarrow}/g_{1r}^{\uparrow\downarrow}) J_S^{sp}(0)$$
$$= \frac{\hbar\omega p g_{1\text{eff}}^{\uparrow\downarrow}}{4\pi} \left(\frac{h}{\Delta H}\right)^2 L(H - H_R), \qquad (21)$$

where $g_{1\text{eff}}^{\uparrow\downarrow}$ is the real part of the effective spin-mixing conductance given by $g_{1\text{eff}}^{\uparrow\downarrow} = g_{1r}^{\uparrow\downarrow}[1 + \beta g_{1r}^{\uparrow\downarrow}]^{-1}$. Equation (21) provides the input for the first boundary condition at $y = 0$. The second boundary condition at $y = d$ results from the fact that the spin current in the NM is produced by the spin pumping from the magnon accumulation in the AFI. The same reasoning used to calculate the spin pumping current from the AFI into the FM can be used here to show that the spin current at the AFI/NM interface is given by

$$J_S(d^+) = b\hbar g_{2\text{eff}}^{\uparrow\downarrow} \delta n_m(d). \qquad (22)$$

where $g_{2\text{eff}}^{\uparrow\downarrow}$ is the effective spin-mixing conductance of the AFI/NM interface that takes into account the backflow spin current from the spin accumulation in the NM [7,8]. Using in Eq. (22) the expression for the magnon accumulation in Eq. (17) and with Eq. (20) we obtain

$$J_S(d) = \frac{c}{\sinh(d/l_m) + c\cosh(d/l_m)} J_S(0), \qquad (23)$$

where c is a dimensionless parameter defined by

$$c = \frac{l_m}{D_m} b g_{2\text{eff}}^{\uparrow\downarrow}. \qquad (24)$$

Using the result in Eq. (23) in Eq. (17) for $y = 0$ we obtain the magnon accumulation at the FM/AFI interface,

$$\delta n_m(0) = \frac{l_m}{\hbar D_m} \left[\frac{1 + c\tanh(d/l_m)}{c + \tanh(d/l_m)}\right] J_S(0). \qquad (25)$$

With this result in Eq. (20) we find for the backflow factor at the FM/AFI interface

$$\beta = \frac{l_m b}{D_m} \left[\frac{1 + c\tanh(d/l_m)}{c + \tanh(d/l_m)}\right]. \qquad (26)$$

As expected, this gives an effective spin-mixing conductance of the FM/AFI interface that depends on the AFI layer thickness,

$$g_{1\text{eff}}^{\uparrow\downarrow}(d) = g_{1r}^{\uparrow\downarrow} \left\{1 + g_{1r}^{\uparrow\downarrow} \frac{l_m b}{D_m} \left[\frac{1 + c\tanh(d/l_m)}{c + \tanh(d/l_m)}\right]\right\}^{-1}. \qquad (27)$$

At this point it is important to check the value of $g_{1\text{eff}}^{\uparrow\downarrow}$ in the limit of vanishing AFI layer thickness. With $d = 0$ Eq. (27) gives

$$\frac{1}{g_{1\text{eff}}^{\uparrow\downarrow}(0)} = \frac{1}{g_{2\text{eff}}^{\uparrow\downarrow}} + \frac{1}{g_{1r}^{\uparrow\downarrow}}, \qquad (28)$$

which is a result similar to the one obtained for the well studied FM/NM/FM trilayer [7,8] and that suffers from the same drawback; namely, the spin-mixing conductance for the FM/NM bilayer without the AFI layer is tied to the values for the FM/AFI and AFI/NM interfaces, which is nonphysical. In the case of the FM/NM/FM trilayer this inconsistency is solved by adding to Eq. (28) a dimensionless resistance to the intermediate NM layer [7,8]. Here we add a dimensionless parameter δ in Eq. (27) so that its value can be adjusted to the one of the FM/NM interface in the limit of $d \to 0$. Thus we use for the spin-mixing conductance of the FM/AFI interface

$$g_{1\text{eff}}^{\uparrow\downarrow}(d) = g_{1r}^{\uparrow\downarrow} \left\{\delta + \frac{c + \tanh(d/l_m)}{c(1 + r) + (1 + rc^2)\tanh(d/l_m)}\right\}, \qquad (29)$$

where $r = g_{1r}^{\uparrow\downarrow}/g_{2\text{eff}}^{\uparrow\downarrow}$. For $d = 0$ this gives $g_{1\text{eff}}^{\uparrow\downarrow}(0) = g_{1r}^{\uparrow\downarrow}[\delta + g_{2\text{eff}}^{\uparrow\downarrow}/(g_{1r}^{\uparrow\downarrow} + g_{2\text{eff}}^{\uparrow\downarrow})]$ so that its value can be adjusted to the actual spin-mixing conductance of the FM/NM interface. In the experiments of Refs. [35–37], the voltage is measured at the edges of the NM layer as a function of the AFI layer thickness d and expressed in terms of the voltage with $d = 0$. Since the voltages are proportional to the spin current density at the AFI/NM interface, we use Eqs. (23) and (29) to write

$$\frac{V(d)}{V(0)} = \frac{c(1 + r)}{1 + \delta(1 + r)} \left[\delta + \frac{c + \tanh(d/l_m)}{c(1 + r) + (1 + rc^2)\tanh(d/l_m)}\right]$$
$$\times \frac{1}{[\sinh(d/l_m) + c\cosh(d/l_m)]}. \qquad (30)$$

This is the quantity that has to be compared with the experimental data. It is valid for a FM/AFI/NM trilayer with any antiferromagnet. In the next section it is evaluated for the YIG/NiO/Pt trilayer investigated experimentally [35–37].

IV. APPLICATION TO YIG/NiO/Pt TRILAYER

In order to compare the results of the diffusive magnonic spin-transport model with experimental results for a specific AFI one needs detailed information on the dispersion relations and relaxation rates for the two magnon modes. They are used to calculate the integrals over the Brillouin zone that appear in the relevant parameters, such as the diffusion coefficient in Eq. (12) and the spin pumping parameter in Eq. (B11). In a hard-axis AF, such as NiO, the magnon frequencies in Eqs. (A26) and (A27) are

$$\omega_{\alpha k} = \gamma \big[H_E(H_{Ax} + H_{Ay}) + H_{Ax}H_{Ay}$$
$$+ \gamma_k H_E(H_{Ax} - H_{Ay}) + H_E^2(1 - \gamma_k^2) \big]^{1/2}, \qquad (31)$$

$$\omega_{\beta k} = \gamma \big[H_E(H_{Ax} + H_{Ay}) + H_{Ax}H_{Ay}$$
$$- \gamma_k H_E(H_{Ax} - H_{Ay}) + H_E^2(1 - \gamma_k^2) \big]^{1/2}, \qquad (32)$$
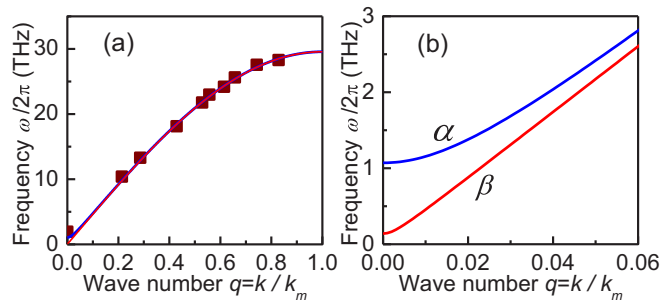
FIG. 2. Spin-wave dispersion in antiferromagnetic NiO at $T = 300$ K. (a) Solid curves show the magnon frequencies calculated with Eqs. (31) and (32). Symbols represent the neutron scattering data of Ref. [59]. (b) Blowup of the Brillouin zone center showing the separation of the frequencies of the α (upper blue curve) and β (lower red curve) magnon modes.

where H_E, H_{Ax}, and H_{Ay} are the exchange, hard-axis anisotropy, and in-plane anisotropy effective fields, respectively; $\gamma = g\mu_B/\hbar$ is the gyromagnetic ratio; g is the spectroscopic splitting factor; and γ_k is the structure factor. As shown in Appendix A, the values of the parameters for NiO can be obtained by fitting Eqs. (31) and (32) to the experimental data [59–61]. Figure 2 shows the calculated dispersion relations for zero external field and $T = 300$ K. We assume a spherical Brillouin zone with a structure factor $\gamma_k = \cos(\pi k/2k_m)$, where $k_m = \pi/a_l$, a_l being the lattice parameter, and use the following parameters: $H_E = 9684$ kOe, $H_{Ax} = 6.35$ kOe, $H_{Ax} = 0.11$ kOe, and $g = 2.18$. The magnon frequencies over the whole Brillouin zone are shown in Fig. 2(a) as a function of the reduced wave number $q = k/k_m$. The separation between the curves for the two modes barely can be seen in Fig. 2(a) but it is very clear in Fig. 2(b) showing a blowup near the zone center. Note that in MnF_2 at zero field the two modes have the same frequency, varying from 260 GHz at the zone center to 1.6 THz at the zone boundary [62]. Similarly, in FeF_2 at zero field the modes are degenerate with frequencies that vary from 1.6 to 2.5 THz [63,64]. Thus, in order to have a sizable separation in the magnon frequencies in MnF_2 and FeF_2 it is necessary to apply a field of tens of kOe [49]. In NiO the frequency reaches 29.5 THz at the zone boundary due to the very large exchange field. But a most important fact is that in the region $q < 0.1$ the two modes have different frequencies and consequently different thermal populations. Thus in NiO the spin currents carried by the two magnon modes do not cancel out in the absence of an external field, in contrast to MnF_2 and Cr_2O_3 [33,34,50] that require the application of a large magnetic field to enable magnonic spin transport. Notice that the FMR experiments of Refs. [35–38] are done in a magnetic field in the range 2–3 kOe. When applied in the direction of the spin alignment in NiO, the effect of the field is simply to shift the magnon frequencies by less than 10 GHz. This is negligible compared to the frequencies in zero field and for this reason the effect of the field is not considered here.

The calculations of the diffusion parameter in Eq. (12) and the spin pumping coefficient in Eq. (B11) are done by expressing all integrals in terms of dimensionless quantities.

One can show that Eq. (12) can be written as

$$D_m = \frac{\pi^2 \tau_0 \hbar^2 \gamma^4 H_E^4}{12 k_m^2 (k_B T)^2} \frac{(B_{1\beta} - B_{1\alpha})}{(B_{0\beta} - B_{0\alpha})}, \tag{33}$$

where τ_0 is the relaxation time of the $k = 0$ magnon and the parameters B are given by the integrals

$$B_{0\alpha} = \int dq\, q^2 \frac{x_\alpha}{e^{x_\alpha} - 1} \quad B_{0\beta} = \int dq\, q^2 \frac{v_{\beta q}}{v_{\alpha q}} \frac{x_\beta}{e^{x_\beta} - 1}, \tag{34}$$

$$B_{1\alpha} = \int dq\, q^2 \frac{\sin^2(\pi q/2)}{x_{\alpha k}\eta_{\alpha q}(e^{x_\alpha} - 1)}$$
$$\times \{-[(H_{Ax} - H_{Ay})/(2H_E)] + \cos(\pi q/2)\}^2, \tag{35}$$

$$B_{1\beta} = \int dq\, q^2 \frac{\sin^2(\pi q/2)}{x_{\beta k}\eta_{\beta q}(e^{x_\beta} - 1)}$$
$$\times \{[(H_{Ax} - H_{Ay})/(2H_E)] + \cos(\pi q/2)\}^2, \tag{36}$$

where $x_\mu = \hbar\omega_{\mu k}/(k_B T)$ is the dimensionless reduced energy, $\eta_{\mu q} = \eta_{\mu k}/\tau_0$ is the k dependent dimensionless relaxation rate relative to the $k = 0$ magnon, and $v_{\mu q}$ is the group velocity calculated with $v_{\mu k} = \partial\omega_{\mu k}/\partial k$ from Eqs. (31) and (32), given by

$$v_{\alpha k} = \gamma^2 \frac{\pi \sin(\pi q/2)}{4 k_m \omega_{\alpha k}} \big[-H_E(H_{Ax} - H_{Ay}) + 2H_E^2 \cos(\pi q/2)\big], \tag{37}$$

$$v_{\beta k} = \gamma^2 \frac{\pi \sin(\pi q/2)}{4 k_m \omega_{\beta k}} \big[H_E(H_{Ax} - H_{Ay}) + 2H_E^2 \cos(\pi q/2)\big]. \tag{38}$$

The integrals in Eqs. (34)–(36) were evaluated numerically with the parameters of NiO and using the relaxation rate at $T = 300$ K of Eq. (A29) written as

$$\eta_k = \eta_0[1 + (1240q + 5860q^3)], \tag{39}$$

where the relaxation rate of the $k = 0$ mode is $\eta_0 = 1/\tau_0 = 1.5 \times 10^9$ s^{-1} as reported in Ref. [61]. As shown in Fig. 3 the integrands of $B_{1\alpha}$ and $B_{1\beta}$ in Eqs. (35) and (36) are zero for $q = 0$ due to the vanishing of the density of states, increase
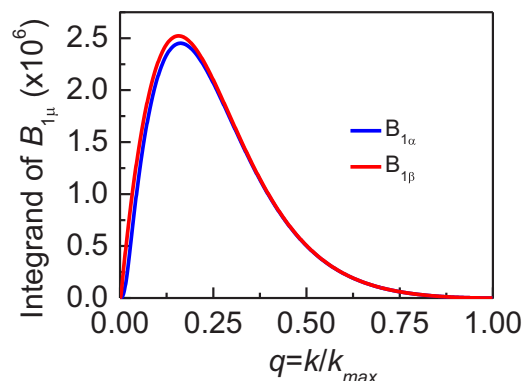

FIG. 3. Integrands of the integrals in Eqs. (35) and (36) for the two magnon modes in NiO at $T = 300$ K.

rapidly with increasing q, reach a peak at $q \approx 0.15$, and fall fast for higher q because the thermal magnon number decreases exponentially with increasing frequency. For $q < 0.25$ the integrand of $B_{1\beta}$ is larger than in $B_{1\alpha}$ because the β magnon mode has smaller frequency, thus a larger thermal occupation number, and larger group velocity than the α mode. The integrations lead to $B_{0\alpha} = 2.59 \times 10^{-2}$, $B_{0\beta} = 2.62 \times 10^{-2}$, $B_{1\alpha} = 8.15 \times 10^{-7}$, and $B_{1\beta} = 8.52 \times 10^{-7}$. Using these values in Eq. (33) and the lattice parameter $a_l = 0.417$ nm for NiO, we obtain for the diffusion parameter $D_m = 9.5 \, \mathrm{cm^2/s}$. This is about one order of magnitude smaller than the value for ferrimagnetic yttrium iron garnet at $T = 300$ K [53,54]. With the diffusion parameter one obtains the magnon-phonon relaxation time τ_{mp} that enters in Eq. (13) through the relation $\tau_{mp} = l_m^2/D_m$. Using for the diffusion length the value $l_m \approx 10$ nm estimated in Ref. [37] we obtain for NiO at $T = 300$ K, $\tau_{mp} \approx 10^{-13}$ s, which is one order of magnitude smaller than in YIG.

The integrals entering in the spin pumping parameter are calculated in a similar manner. From Eq. (B11) one can write the spin pumping coefficient as

$$b = \frac{a_l^3 k_B T}{2\pi^2 \hbar} \frac{(B_{2\beta} - B_{2\alpha})}{(B_{0\beta} - B_{0\alpha})}, \tag{40}$$

where the new integrals are given approximately by

$$B_{2\alpha} = \int dq \, q^2 \left(\frac{\gamma H_E}{\omega_k} \right) n_{\alpha k}^0 x_{\alpha k}^2, \tag{41}$$

$$B_{2\beta} = \int dq \, q^2 \left(\frac{\gamma H_E}{\omega_k} \right) \rho_k n_{\beta k}^0 x_{\beta k}^2, \tag{42}$$

where $\omega_k = \omega_{\beta k} \approx \omega_{\alpha k}$ in the region $q > 0.2$ that contributes mostly to the integrals. Numerical integration with the parameters for NiO gives $B_{2\alpha} = 0.1226$ and $B_{2\beta} = 0.1237$. With these values and the factor in Eq. (40) we get $b \approx 7 \times 10^{-10} \, \mathrm{cm^3 \, s^{-1}}$. We can now obtain a value for the relevant parameter c in Eq. (24). For this we use the calculated diffusion parameter $D_m = 9.5 \, \mathrm{cm^2/s}$, the estimated diffusion length $l_m \approx 10$ nm [37], and a spin-mixing conductance for the NiO/Pt interface similar to the one for YIG/Pt, $g_{2\mathrm{eff}}^{\uparrow\downarrow} \approx 10^{15} \, \mathrm{cm^{-2}}$ [5,6]. With Eq. (24) we obtain $c \approx 8 \times 10^{-2}$.

Having the value for the important parameter c that contains information on the AFI and the AFI/NM interface, we are in the position to compare the model with the experimental results. The measured dependence of the voltage on the AFI thickness is fit with Eq. (30) allowing the four adjustable parameters to vary in the following ranges: $c = [0, 1], r = [1, 10], \delta = [-5, +5], l_m = [5, 15]$ nm. Figure 4 shows the least-squares deviation fit to the data of Ref. [37], obtained with the following parameters: $c = 0.1$, $r = 4.2$, $\delta = -0.15$, and $l_m = 7.4$ nm. The value of the parameter c obtained from the fit is in excellent agreement with the one calculated for NiO. The diffusion length is also very close to the value of 9.8 nm obtained from the fit of an exponential variation to the experimental data [37]. From the value of the ratio r obtained from the fit we find that $g_{\mathrm{YIG/NiO}}^{\uparrow\downarrow} = 4.2 g_{\mathrm{NiO/Pt}}^{\uparrow\downarrow}$. This result provides a physical explanation for the initial increase of the voltage with increasing AFI thickness. The coupling of the spin excitations at the YIG/NiO interface is larger than in NiO/Pt and in YIG/Pt, so that when a NiO layer is introduced between YIG and
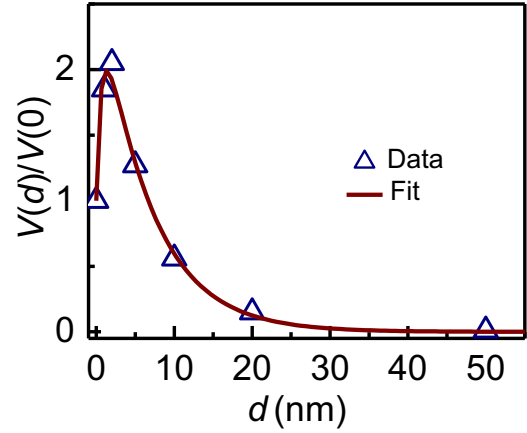

FIG. 4. Voltage measured at the Pt layer in YIG/NiO(d)/Pt trilayers as a function of the NiO layer thickness. The symbols represent the experimental data of Ref. [37] and the curve represents the best fit with Eq. (30).

Pt, the spin current pumped by the magnetization precession in YIG increases. Of course, as the thickness of the NiO increases the spin current tends to decrease due to magnon diffusion and loss of spin angular momentum to the lattice. The overall behavior of the voltage with increasing d is the peak followed by an exponential decay as in Fig. 4. Finally we note that for $d \gg l_m$ the dependence of the voltage on the AFI thickness is $V(d) \propto \exp(-d/l_m)$, as assumed in Ref. [37]. However, this exponential decay breaks down for thickness smaller or comparable to the magnon diffusion thickness, as demonstrated here.

In summary, we have presented a model for the spin transport in an antiferromagnetic insulator based on the diffusion of thermal magnons. In easy-axis AFs such as MnF_2, FeF_2 and Cr_2O_3, in the absence of an external magnetic field the spin currents carried by the two magnon modes cancel out. However, in the room-temperature AFI NiO, even in zero field, the two magnon modes have different frequencies and hence different thermal populations, so that magnonic spin transport is made possible. We have shown that in a FM/AFI/NM structure with the FM layer under ferromagnetic resonance, the spin current pumped into the AFI is carried by the diffusion of magnons. Solution of the spin current boundary-value problem for the trilayer yields an expression for the voltage detected in the NM layer that depends on the thickness of the AFI layer and on the spin-mixing conductance of the two interfaces. We have used in the model the magnon diffusion and spin pumping properties of NiO calculated based on the actual magnon dispersions and damping rates. The calculated dependence of the voltage on the AFI layer thickness is in quite good quantitative agreement with the experimental data of Refs. [35–37].

APPENDIX A: SPIN WAVES IN THE HARD-AXIS ANTIFERROMAGNET NiO

Nickel oxide is a prototype two-sublattice hard-axis anti-ferromagnet with Néel temperature $T_N = 523$ K. It has a fcc crystal structure with a hard-axis anisotropy perpendicular to (111) planes [59]. At temperatures below T_N the spins of one sublattice are aligned along $\langle 11\bar{2} \rangle$ directions in (111) planes and the spins of the other sublattice are oppositely aligned in neighboring (111) planes. In the absence of an applied magnetic field, the spin Hamiltonian with exchange interaction and out-of-plane (x) and in-plane (y) anisotropy energies can be written as [59]

$$\text{H} = \sum_{i \neq j} 2J_{ij}\vec{S}_i \cdot \vec{S}_j + \sum_i D_x (S_i^x)^2 + D_y (S_i^y)^2, \quad \text{(A1)}$$

where z is the direction of spin alignment; $\vec{S}_i$ is the spin (in units of $\hbar$) at a generic lattice site i; J_{ij} is the exchange constant of the interaction between spins $\vec{S}_i$ and $\vec{S}_j$; D_x and D_y are, respectively, the anisotropy constants in the hard direction and in the plane. We treat the quantized excitations of the magnetic system with the approach of Holstein-Primakoff [65], which consists of transformations that express the spin operators in terms of boson operators that create or destroy magnons. In the first transformation the components of the local spin operators are related to the creation and annihilation operators of spin deviations at site i. Since there are two sublattices we introduce different spin deviation operators for each sublattice. Denoting the spins of the up and down sublattices by subscripts 1 and 2, respectively, we have in the linear approximation [65]

$$S_{1i}^+ = (2S)^{1/2}a_i, \;\; S_{1i}^- = (2S)^{1/2}a_i^\dagger, \;\; S_{1i}^z = S - a_i^\dagger a_i, \quad \text{(A2)}$$

$$S_{2i}^+ = (2S)^{1/2}b_i^\dagger, \;\; S_{2i}^- = (2S)^{1/2}b_i, \;\; S_{2i}^z = -S + b_i^\dagger b_i, \quad \text{(A3)}$$

where $a_i^\dagger$, a_i and $b_i^\dagger$, b_i are the creation, destruction operators for spin deviations at sites 1 and 2, which satisfy the boson commutation rules $[a_i, a_j^\dagger] = \delta_{ij}$, $[a_i, a_j] = 0$, $[b_i, b_j^\dagger] = \delta_{ij}$, and $[b_i, b_j] = 0$. The next step consists in introducing a transformation from the localized field operators to collective boson operators that satisfy the commutation rules $[a_k, a_{k'}^\dagger] = \delta_{kk'}$, $[a_k, a_{k'}] = 0$, $[b_k, b_{k'}^\dagger] = \delta_{kk'}$, $[b_k, b_{k'}] = 0$,

$$a_i = N^{-1/2}\sum_k e^{i\vec{k}\cdot\vec{r}_i}a_k, \;\; b_i = N^{-1/2}\sum_k e^{i\vec{k}\cdot\vec{r}_i}b_k, \quad \text{(A4)}$$

where N is the number of spins in each sublattice and $\vec{k}$ is a wave vector. Using Eq. (A4) in Eqs. (A2) and (A3) one can write the Hamiltonian quadratic in boson operators in the form

$$\text{H} = \hbar \sum_k A_k(a_k^\dagger a_k + b_k^\dagger b_k) + B_k(a_k b_{-k} + a_k^\dagger b_{-k}^\dagger)$$

$$+ \frac{1}{2}C_k(a_k a_{-k} + b_k b_{-k} + \text{H.c.}), \quad \text{(A5)}$$

where

$$A_k = \gamma[H_E + (H_{Ax} + H_{Ay})/2], \quad \text{(A6)}$$

$$B_k = \gamma\gamma_k H_E, \;\; \gamma_k = (1/z)\sum_\delta \exp(i\vec{k}\cdot\vec{\delta}), \quad \text{(A7)}$$

$$C_k = \gamma(H_{Ax} - H_{Ay}). \quad \text{(A8)}$$

We have considered only intersublattice exchange interaction between the z nearest neighbors with parameter J and defined the effective exchange and anisotropy fields as

$$H_E = 2SzJ/\gamma\hbar, \quad H_{Ax} = 2SD_x/\gamma\hbar, \quad H_{Ay} = 2SD_y/\gamma\hbar, \quad \text{(A9)}$$

where $\gamma = g\mu_B/\hbar$ is the gyromagnetic ratio, g is the spectroscopic splitting factor, μ_B the Bohr magneton, and $\hbar$ the reduced Planck constant. We wish to find a transformation to normal mode magnon creation and destruction operators $\alpha_k^\dagger$, α_k and $\beta_k^\dagger$, β_k that leads the Hamiltonian to the diagonal form

$$\text{H} = \sum_k \hbar(\omega_{\alpha k}\alpha_k^\dagger \alpha_k + \omega_{\beta k}\beta_k^\dagger \beta_k), \quad \text{(A10)}$$

where $\omega_{\alpha k}$ and $\omega_{\beta k}$ are the frequencies of the two magnon modes. We follow White *et al.* [66] and write Eq. (A5) in matrix form

$$\text{H} = \hbar \sum_{k>0} \text{H}_k, \;\; \text{H}_k = (X)^\dagger[\text{H}](X), \quad \text{(A11)}$$

where the matrices are

$$(X) = \begin{pmatrix} a_k \\ b_{-k}^\dagger \\ a_{-k}^\dagger \\ b_k \end{pmatrix}, \quad [\text{H}] = \hbar \begin{pmatrix} A_k & B_k & C_k & 0 \\ B_k & A_k & 0 & C_k \\ C_k & 0 & A_k & B_k \\ 0 & C_k & B_k & A_k \end{pmatrix}. \quad \text{(A12)}$$

The next step consists of introducing a linear transformation to new operators

$$(X) = [Q](Z), \;\; (Z) = \begin{pmatrix} \alpha_k \\ \beta_{-k}^\dagger \\ \alpha_{-k}^\dagger \\ \beta_k \end{pmatrix}, \quad \text{(A13)}$$

such that the Hamiltonian in Eq. (A11) can be written as

$$\text{H} = \hbar \sum_k (Z)^\dagger[\omega](Z), \quad \text{(A14)}$$

where $[\omega]$ is a diagonal eigenvalue matrix. In order to find the transformation matrix $[Q]$ one needs a few relations. The first follows from the introduction of (A13) in (A11) and comparison with (A14). This leads to

$$[Q]^\dagger[\text{H}][Q] = \hbar[\omega]. \quad \text{(A15)}$$

Another relation is obtained from the boson commutation rules. They can be written in matrix forms

$$[X, X^\dagger] = X(X)^\dagger - (X^*X^T)^T = g, \quad \text{(A16)}$$

$$[Z, Z^\dagger] = Z(Z)^\dagger - (Z^*Z^T)^T = g, \quad \text{(A17)}$$

where

$$g = \begin{pmatrix} 1 & 0 & 0 & 0 \\ 0 & -1 & 0 & 0 \\ 0 & 0 & -1 & 0 \\ 0 & 0 & 0 & 1 \end{pmatrix}. \qquad (A18)$$

Using Eq. (A13) in (A16) and in (A17) we obtain an orthonormality relation for the transformation matrix,

$$[Q][g][Q]^{\dagger} = [g]. \qquad (A19)$$

With (16)–(A19) one obtains an eigenvalue equation

$$[H][Q] = [g]^{-1}[Q][g]\hbar[\omega]. \qquad (A20)$$

Solution of Eq. (A20) yields the elements of the transformation matrix and the frequencies of the two magnon modes,

$$\omega_{\alpha k}^2 = A_k^2 - (B_k - C_k)^2, \qquad (A21)$$

$$\omega_{\beta k}^2 = A_k^2 - (B_k + C_k)^2. \qquad (A22)$$

Note that since $(S_i^x)^2 + (S_i^y)^2 = S^2 - (S_i^z)^2$, if $D_x = D_y$ the anisotropy becomes easy axis in the z direction, with $H_A = 2SD_x/g\mu_B$ and $C_k = 0$. In this case the two magnon frequencies are $\omega_{\alpha k}^2 = \omega_{\beta k}^2 = \omega_k^2 = A_k^2 - B_k^2$, where

$$\omega_k = \pm\gamma\left[2H_E H_A + H_A^2 + H_E^2\left(1 - \gamma_k^2\right)\right]^{1/2}, \quad (A23)$$

which is the known result for the AF with easy-axis anisotropy and no applied external field [49]. In this case the transformation of the magnon operators is

$$a_k = u_k \alpha_k - v_k \beta_{-k}^{\dagger}, \qquad (A24a)$$

$$b_{-k}^{\dagger} = -v_k \alpha_k + u_k \beta_{-k}^{\dagger}, \qquad (A24b)$$

where

$$u_k = [(A_k + \omega_k)/2\omega_k]^{1/2}, \quad v_k = [(A_k - \omega_k)/2\omega_k]^{1/2}. \qquad (A25)$$

The transformation coefficients satisfy the orthonormality condition $u_k^2 - v_k^2 = 1$. In NiO the parameter C_k is very small compared to the others, $C_k \approx 10^{-3}A_k$, so that in most parts of the Brillouin zone the two frequencies are approximately the same and the transformation of the magnon operators is approximately given by Eq. (A24) [66,67].

Using the relations (A6)–(A8) in (A21) and (A22) one can write the frequencies of the two magnon modes in terms of the effective fields,

$$\omega_{\alpha k}^2 = \gamma^2\big[H_E(H_{Ax} + H_{Ay}) + H_{Ax}H_{Ay} + \gamma_k H_E(H_{Ax} - H_{Ay}) + H_E^2\big(1 - \gamma_k^2\big)\big], \quad (A26)$$

$$\omega_{\beta k}^2 = \gamma^2\big[H_E(H_{Ax} + H_{Ay}) + H_{Ax}H_{Ay} - \gamma_k H_E(H_{Ax} - H_{Ay}) + H_E^2\big(1 - \gamma_k^2\big)\big]. \quad (A27)$$

For $H_E \gg H_{Ax}, H_{Ay}$, the frequencies of the zone center $k = 0$ ($\gamma_k = 1$) magnons are

$$\omega_{\alpha 0} \approx \gamma(2H_{Ax}H_E)^{1/2}, \quad \omega_{\beta 0} \approx \gamma(2H_{Ay}H_E)^{1/2}. \quad (A28)$$

The magnetic parameters for NiO are determined by fitting the calculated frequencies in (A26) and (A27) to three sets of data. Fitting to the neutron scattering measurements of Hutchings and Samuelsen [59] gives the value of the exchange field $H_E = 9684$ kOe considering for the g factor $g = 2.18$. Since the neutron data do not have sufficient resolution to determine the frequencies of the zone-center magnons, we use the value $\omega_{\beta 0}/2\pi = 0.140$ THz measured by Brillouin light scattering [60] and $\omega_{\alpha 0}/2\pi = 1.07$ THz obtained from magnetization oscillations in the far infrared [61]. With these values in (A28) we determine the anisotropy fields, $H_{Ax} = 6.35$ kOe and $H_{Ay} = 0.11$ kOe. Figure 2 shows the dispersion relations calculated with Eqs. (A26) and (A27) assuming a spherical Brillouin zone and using for the structure factor $\gamma_k = \cos(\pi k/2k_m)$, where $k_m = \pi/a_l$, a_l being the lattice parameter.

In order to calculate the diffusion parameter it is necessary to have the lifetime of magnons as a function of the wave number. The lifetime of α mode with $k = 0$ has been measured in NiO from the decay time of the magnetization oscillations [61]. However, there are no damping data for the magnons with wave numbers in the range $q = 0.1 - 0.5$ that dominate the integrals in Eqs. (35) and (36) at room temperature. Thus we have calculated the spin-wave relaxation due to four-magnon processes that are known to explain the experimental data in other antiferromagnets [68,69]. The calculation is done numerically by integrations over a spherical Brillouin zone of the transition probability for four-magnon scattering at a fixed temperature T and varying the wave number k [68,69]. Figure 5 shows the calculated relaxation rate for magnons in NiO as a function of the wave number for $T = 300$ K using the parameters obtained from the fit to data of the calculated magnon frequencies as explained earlier. We use for the residual damping at $k = 0$ the value obtained from the Gilbert damping parameter $\alpha = 2.1 \times 10^{-4}$ measured in Ref. [61] for the mode at 1.1 THz. Figure 5 also shows a polynomial fit to the calculated four-magnon relaxation rate
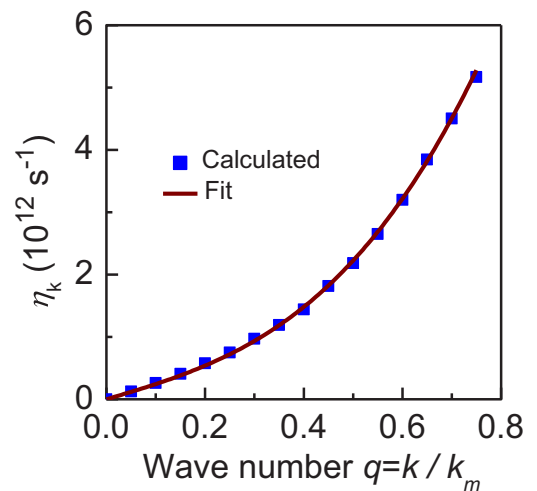

FIG. 5. Magnon relaxation rate in antiferromagnetic NiO. Symbols represent the calculation with four-magnon scattering processes at $T = 300$ K while the solid line is the polynomial fit with Eq. (A29).

with the residual damping described by

$$\eta_k = 1.5 \times 10^9 + (2.35q + 8.3q^3) \times 10^{12} \, \text{s}^{-1}. \quad \text{(A29)}$$

This is the expression used to evaluate the integrals in Eqs. (35) and (36).

APPENDIX B: SPIN CURRENT AND SPIN PUMPING IN NiO

Initially we derive an expression for the spin current carried by magnons in a hard-axis antiferromagnet simply by considering that it expresses the flow of angular momentum. The total z component of the spin angular momentum carried by magnons is given by $S^z = \sum_i (S_{1i}^z + S_{2i}^z)$. With Eqs. (A2)–(A4) one can write the z component of the spin angular momentum as

$$S^z = \sum_k -a_k^\dagger a_k + b_k^\dagger b_k. \quad \text{(B1)}$$

Using the transformation to the magnon operators given by (A24) and keeping only terms with magnon number operators we have

$$S^z = \sum_k (-\alpha_k^\dagger \alpha_k + \beta_k^\dagger \beta_k). \quad \text{(B2)}$$

The opposite signs in the angular momenta of the two modes is consistent with the semiclassical picture of the spins precessing in opposite directions. Considering for each mode μ the group velocity $\vec{v}_{\mu k} = \hat{k} \partial \omega_\mu / \partial k$, the spin current density operator is

$$\vec{J}_S^z = \frac{\hbar}{V} \sum_k [-\vec{v}_{\alpha k} \alpha_k^\dagger \alpha_k + \vec{v}_{\beta k} \beta_k^\dagger \beta_k], \quad \text{(B3)}$$

which is the same expression derived for easy-axis antiferromagnets [47].

The spin pumping from coherent magnetization precession in an antiferromagnet has been studied by Cheng *et al.* [56] using a semiclassical approach. Here we calculate the spin pumping from thermal magnon accumulation in an AFI using a quantum formulation based on the transformation of the spin variables into magnon operators. In terms of the magnetizations of the two sublattices $\vec{M}_1$, $\vec{M}_2$ the spin current pumped by an AFI into an adjacent NM layer is at the interface [7,8,56],

$$\vec{J}_S^{sp} = \left(\frac{\hbar g_r^{\uparrow\downarrow}}{4\pi M_1^2} \vec{M}_1 \times \frac{d\vec{M}_1}{dt} + \frac{\hbar g_r^{\uparrow\downarrow}}{4\pi M_2^2} \vec{M}_2 \times \frac{d\vec{M}_2}{dt} \right), \quad \text{(B4)}$$

where $g_r^{\uparrow\downarrow}$ is the real part of the spin-mixing conductance of the interface. From Eq. (B4) one can show that the z component of the spin current pumped by the precessing magnetization of

the AFI sublattices is given by

$$J_{S_y}^z = \frac{\hbar g_r^{\uparrow\downarrow}}{4\pi M^2} \frac{1}{2i} \left(-m_1^+ \frac{dm_1^-}{dt} \right.$$
$$\left. + m_1^- \frac{dm_1^+}{dt} - m_2^+ \frac{dm_2^-}{dt} + m_2^- \frac{dm_2^+}{dt} \right), \quad \text{(B5)}$$

where m_1^+ and m_1^- are the transverse circularly polarized components of the magnetization of the up sublattice, related to the spin deviation operators by Eq. (A2),

$$m_1^+ = (\gamma\hbar/V)\sqrt{2S} \sum_i a_i, \quad m_1^- = (\gamma\hbar/V)\sqrt{2S} \sum_i a_i^\dagger. \quad \text{(B6)}$$

Similarly, for the down sublattice we have

$$m_2^+ = (\gamma\hbar/V)\sqrt{2S} \sum_i b_i^\dagger, \quad m_2^- = (\gamma\hbar/V)\sqrt{2S} \sum_i b_i. \quad \text{(B7)}$$

Using (B6) and (B7) in (B5), replacing the spin deviation operators by magnon operators by means of transformations (A4) and (A24), and keeping only terms with magnon number operators we obtain for the z component of the spin current density pumped at the interface

$$J_S^z = \frac{\gamma\hbar^2 g_r^{\uparrow\downarrow}}{2\pi M V} \sum_k (u_k^2 + v_k^2)(-\omega_{\alpha k} \alpha_k^\dagger \alpha_k + \omega_{\beta k} \beta_k^\dagger \beta_k). \quad \text{(B8)}$$

Replacing the sum on the wave number by an integral over the Brillouin zone in the usual way, considering for expectation values of the magnon numbers the numbers in excess of equilibrium, and using (A25) we obtain

$$J_S^z = -\frac{\gamma\hbar^2 g_r^{\uparrow\downarrow}}{2\pi M (2\pi)^3} \int d^3k \left(\frac{A_k}{\omega_k} \right) (\delta n_{\alpha k} \omega_{\alpha k} - \delta n_{\beta k} \omega_{\beta k}). \quad \text{(B9)}$$

With Eq. (8) this becomes

$$J_S^z = -\frac{\gamma\hbar^2 g_r^{\uparrow\downarrow}}{2\pi M (2\pi)^3} \int d^3k \left(\frac{A_k}{\omega_k} \right)$$
$$\times (n_{\alpha k}^0 \varepsilon_{k\alpha} \omega_{\alpha k} - n_{\beta k}^0 \varepsilon_{k\beta} \omega_{\beta k}) g(y).$$

Finally, using Eqs. (9) and (10) the spin current pumped by thermal magnons in the AF in excess of equilibrium can be written as

$$J_S^z = -b\hbar g_r^{\uparrow\downarrow} \delta n_m(0), \quad \text{(B10)}$$

where

$$b = \frac{\gamma}{(2\pi)^3 2\pi M} \frac{1}{(I_{0\beta} - I_{0\alpha})} \int d^3k \left(\frac{A_k}{\omega_k} \right)$$
$$\times (-n_{\alpha k}^0 \varepsilon_{\alpha k}^2 + \rho_k n_{\beta k}^0 \varepsilon_{\beta k}^2). \quad \text{(B11)}$$

[1] *Spin Current*, edited by S. Maekawa, S. O. Valenzuela, E. Saitoh, and T. Kimura, Series on Semiconductor Science and Technology (Oxford University Press, Oxford, 2012).

[2] *Handbook of Spin Transport in Magnetism*, edited by E. Y. Tsymbal and I. Zutic (CRC Press, Boca Raton, FL, 2012).

[3] J. E. Hirsch, Phys. Rev. Lett. **83**, 1834 (1999).

[4] S. O. Valenzuela and M. Tinkham, Nature **442**, 176 (2006).

[5] A. Hoffmann, IEEE Trans. Magn. **49**, 5172 (2013).

[6] J. Sinova, S. O. Valenzuela, J. Wunderlich, C. H. Back, and T. Jungwirth, Rev. Mod. Phys. **87**, 1213 (2015).

[7] Y. Tserkovnyak, A. Brataas, and G. E. W. Bauer, Phys. Rev. B **66**, 224403 (2002).

[8] Y. Tserkovnyak, A. Brataas, G. E. W. Bauer, and B. I. Halperin, Rev. Mod. Phys. **77**, 1375 (2005).

[9] A. Azevedo, L. H. Vilela Leão, R. L. Rodriguez-Suarez, A. B. Oliveira, and S. M. Rezende, J. Appl. Phys. **97**, 10C715 (2005).

[10] E. Saitoh, M. Ueda, H. Miyajima, and G. Tatara, Appl. Phys. Lett. **88**, 182509 (2006).

[11] K. Uchida, S. Takahashi, K. Harii, J. Ieda, W. Koshibae, K. Ando, S. Maekawa, and E. Saitoh, Nature **455**, 778 (2008).

[12] K. Uchida, J. Xiao, H. Adachi, J. Ohe, S. Takahashi, J. Ieda, T. Ota, Y. Kajiwara, H. Umezawa, H. Kawai, G. E. W. Bauer, S. Maekawa, and E. Saitoh, Nat. Mater. **9**, 894 (2010).

[13] G. E. W. Bauer, E. Saitoh, and B. J. van Wees, Nat. Mater. **11**, 391 (2012).

[14] H. Adachi, K. Uchida, E. Saitoh, and S. Maekawa, Rep. Prog. Phys. **76**, 036501 (2013).

[15] S. R. Boona, R. C. Myers, and J. P. Heremans, Energy Environ. Sci. **7**, 885 (2014).

[16] K. Uchida, M. Ishida, T. Kikkawa, A. Kirihara, T. Murakami, and E. Saitoh, J. Phys.: Condens. Matter **26**, 343202 (2014).

[17] J. C. Rojas Sánchez, L. Vila, G. Desfonds, S. Gambarelli, J. P. Attané, J. M. De Teresa, C. Magén, and A. Fert, Nat. Commun. **4**, 2944 (2013).

[18] K. Shen, G. Vignale, and R. Raimondi, Phys. Rev. Lett. **112**, 096601 (2014).

[19] S. S.-L. Zhang, K. Chen, and S. Zhang, Europhys. Lett. **106**, 67007 (2014).

[20] J. B. S. Mendes, O. Alves Santos, L. M. Meireles, R. G. Lacerda, L. H. Vilela-Leão, F. L. A. Machado, R. L. Rodríguez-Suárez, A. Azevedo, and S. M. Rezende, Phys. Rev. Lett. **115**, 226601 (2015).

[21] E. Padrón-Hernández, A. Azevedo, and S. M. Rezende, Appl. Phys. Lett. **99**, 192511 (2011).

[22] A. Hamadeh, O. d'Allivy Kelly, C. Hahn, H. Meley, R. Bernard, A. H. Molpeceres, V. V. Naletov, M. Viret, A. Anane, V. Cros, S. O. Demokritov, J. L. Prieto, M. Muñoz, G. de Loubens, and O. Klein, Phys. Rev. Lett. **113**, 197203 (2014).

[23] S. Maekawa, H. Adachi, K.-I. Uchida, J. Ieda, and E. Saitoh, J. Phys. Soc. Jpn. **82**, 102002 (2013).

[24] Y. Kajiwara, K. Harii, S. Takahashi, J. Ohe, K. Uchida, M. Mizuguchi, H. Umezawa, H. Kawai, K. Ando, K. Takanashi, S. Maekawa, and E. Saitoh, Nature (London) **464**, 262 (2010).

[25] A. A. Serga, A. V. Chumak, and B. Hillebrands, J. Phys. D: Appl. Phys. **43**, 264002 (2010).

[26] A. V. Chumak, V. I. Vasyuchka, A. A. Serga, and B. Hillebrands, Nat. Phys. **11**, 453 (2015).

[27] S. S. P. Parkin, K. P. Roche, M. G. Samant, P. M. Rice, R. B. Beyers, R. E. Scheuerlein, E. J. O'sullivan, S. L. Brown, J. Bucchigano, D. W. Abraham, Y. Lu, M. Rooks, P. L. Trouilloud, R. A. Wanner, and W. J. Gallagher, J. Appl. Phys. **85**, 5828 (1999).

[28] J. Nogués and I. K. Schuller, J. Magn. Magn. Mater. **192**, 203 (1999).

[29] J. R. Fermin, M. A. Lucena, A. Azevedo, F. M. de Aguiar, and S. M. Rezende, J. Appl. Phys. **87**, 6421 (2000).

[30] T. Jungwirth, X. Marti, P. Wadley, and J. Wunderlich, arXiv:1509.05296 (2015).

[31] J. B. S. Mendes, R. O. Cunha, O. Alves Santos, P. R. T. Ribeiro, F. L. A. Machado, R. L. Rodriguez-Suarez, A. Azevedo, and S. M. Rezende, Phys. Rev. B **89**, 140406(R) (2014).

[32] W. Zhang, M. B. Jungfleisch, W. Jiang, J. E. Pearson, A. Hoffmann, F. Freimuth, and Y. Mokrousov, Phys. Rev. Lett. **113**, 196602 (2014).

[33] S. M. Wu, W. Zhang, Amit K. C., P. Borisov, J. E. Pearson, J. S. Jiang, D. Lederman, A. Hoffmann, and A. Bhattacharya, arXiv:1509.00439 (2015).

[34] S. Seki, T. Ideue, M. Kubota, Y. Kozuka, R. Takagi, M. Nakamura, Y. Kaneko, M. Kawasaki, and Y. Tokura, Phys. Rev. Lett. **115**, 266601 (2015).

[35] H. Wang, C. Du, P. C. Hammel, and F. Yang, Phys. Rev. Lett. **113**, 097202 (2014).

[36] C. Hahn, G. de Loubens, V. V. Naletov, J. Ben Youssef, O. Klein, and M. Viret, Europhys. Lett. **108**, 57005 (2014).

[37] H. Wang, C. Du, P. C. Hammel, and F. Yang, Phys. Rev. B **91**, 220410(R) (2015).

[38] T. Moriyama, S. Takei, M. Nagata, Y. Yoshimura, N. Matsuzaki, T. Terashima, Y. Tserkovnyak, and T. Ono, Appl. Phys. Lett. **106**, 162406 (2015).

[39] A. S. Núñez, R. A. Duine, P. Haney, and A. H. MacDonald, Phys. Rev. B **73**, 214426 (2006).

[40] A. B. Shick, S. Khmelevskyi, O. N. Mryasov, J. Wunderlich, and T. Jungwirth, Phys. Rev. B **81**, 212409 (2010).

[41] A. H. MacDonald and M. Tsoi, Philos. Trans. R. Soc., A **369**, 3098 (2011).

[42] V. M. T. S. Barthem, C. V. Colin, H. Mayaffre, M.-H. Julien, and D. Givord, Nat. Commun. **4**, 2892 (2013).

[43] P. Merodio, A. Ghosh, C. Lemonias, E. Gautier, U. Ebels, M. Chshiev, H. Béa, V. Baltz, and W. E. Bailey, Appl. Phys. Lett. **104**, 032406 (2014).

[44] E. V. Gomonay and V. M. Loktev, Low Temp. Phys. **40**, 17 (2014).

[45] H. Chen, Q. Niu, and A. H. MacDonald, Phys. Rev. Lett. **112**, 017205 (2014).

[46] S. Takei, T. Moriyama, T. Ono, and Y. Tserkovnyak, Phys. Rev. B **92**, 020409(R) (2015).

[47] R. Khymyn, I. Lisenkov, V. S. Tiberkevich, A. N. Slavin, and B. Ivanov, arXiv:1511.05785 (2015).

[48] F. Keffer and C. Kittel, Phys. Rev. **85**, 329 (1952).

[49] S. M. Rezende, R. L. Rodríguez-Suárez, and A. Azevedo, Phys. Rev. B **93**, 014425 (2016).

[50] Y. Ohnuma, H. Adachi, E. Saitoh, and S. Maekawa, Phys. Rev. B **87**, 014423 (2013).

[51] S. S.-L. Zhang and S. Zhang, Phys. Rev. Lett. **109**, 096603 (2012).

[52] S. S.-L. Zhang and S. Zhang, Phys. Rev. B **86**, 214424 (2012).

[53] S. M. Rezende, R. L. Rodríguez-Suárez, R. O. Cunha, A. R. Rodrigues, F. L. A. Machado, G. A. Fonseca Guerra, J. C. López Ortiz, and A. Azevedo, Phys. Rev. B **89**, 014416 (2014).

[54] S. M. Rezende, R. L. Rodríguez-Suárez, J. C. López Ortiz, and A. Azevedo, J. Magn. Magn. Mater. **400**, 171 (2016).

[55] F. Reif, *Fundamentals of Statistical and Thermal Physics* (McGraw-Hill Book Company, New York, 2008).

[56] S. M. Rezende, R. L. Rodríguez-Suárez, and A. Azevedo, Phy. Rev. B **88**, 014404 (2013).

[57] A. Azevedo, L. H. Vilela Leão, R. L. Rodríguez-Suárez, A. F. Lacerda Santos, and S. M. Rezende, Phys. Rev. B **83**, 144402 (2011).

[58] R. Cheng, J. Xiao, Q. Niu, and A. Brataas, Phys. Rev. Lett. **113**, 057601 (2014).

[59] M. T. Hutchings and E. J. Samuelsen, Phys. Rev. B **6**, 3447 (1972).

[60] J. Milano, L. B. Steren, and M. Grimsditch, Phys. Rev. Lett. **93**, 077601 (2004).

[61] T. Kampfrath, A. Sell, G. Klatt, A. Pashkin, S. Mährlein, T. Dekorsy, M. Wolf, M. Fiebig, A. Leitenstorfer, and R. Huber, Nat. Photonics **5**, 31 (2010).

[62] S. P. Bayrakci, T. Keller, K. Habicht, and B. Keimer, Science **312**, 1926 (2006).

[63] M. T. Hutchings, B. D. Rainford, and H. J. Guggenheim, J. Phys. C: Solid State Phys. **3**, 307 (1970).

[64] R. W. Sanders, V. Jaccarino, and S. M. Rezende, Solid State Commun. **28**, 907 (1978).

[65] R. M. White, *Quantum Theory of Magnetism*, 3rd ed. (Springer-Verlag, Berlin, 2007).

[66] R. M. White, M. Sparks, and I. Ortenburger, Phys. Rev. **139**, A450 (1965).

[67] R. B. Woolsey and R. M. White, Int. J. Magn. **2**, 51 (1972).

[68] S. M. Rezende and R. M. White, Phys. Rev. B **14**, 2939 (1976).

[69] S. M. Rezende and R. M. White, Phys. Rev. B **18**, 2346 (1978).